INTEGRATED PRODUCTION SYSTEM OPTIMIZATION USING GLOBAL OPTIMIZATION TECHNIQUES

T. L. Mason, C. Emelle, J. van Berkel

Shell International Production and Exploration B.V
Kesslerpark 1, Postbus 60
2280 AB Rijswijk, The Netherlands

A. M. Bagirov

Centre for Informatics and Applied Optimization,
School of Information Technology and Mathematical Sciences,
University of Ballarat, Ballarat, Victoria, 3353, Australia

F. Kampas

WAM Systems Inc., Plymouth Meeting, PA, USA

J. D. Pintér

PCS Inc., 129 Glenforest Drive, Halifax, NS, Canada B3M 1J2
(Communicated by Kok Lay Teo)

Abstract. Many optimization problems related to integrated oil and gas production systems are nonconvex and multimodal. Additionally, apart from the innate nonsmoothness of many optimization problems, nonsmooth functions such as minimum and maximum functions may be used to model flow/pressure controllers and cascade mass in the gas gathering and blending networks. In this paper we study the application of different versions of the derivative free Discrete Gradient Method (DGM) as well as the Lipschitz Global Optimizer (LGO) suite to production optimization in integrated oil and gas production systems and their comparison with various local and global solvers used with the General Algebraic Modeling System (GAMS). Four nonconvex and nonsmooth test cases were constructed from a small but realistic integrated gas production system optimization problem. The derivation of the system of equations for the various test cases is also presented. Results demonstrate that DGM is especially effective for solving nonsmooth optimization problems and its two versions are capable global optimization algorithms. We also demonstrate that LGO solves successfully the presented test (as well as other related real-world) problems.

1. **Introduction.** It is well recognized that many optimization problems in the oil and gas industry are global optimization problems. They may have a large number of decision variables and the objective and/or constraint functions in these problems may contain nonsmooth functions such as maximum, minimum functions and if statements. The presence of such functions leads to nonsmooth and even to discontinuous optimization problem.

So far, different meta-heuristics such as genetic algorithms (GA) and simulated annealing (SA) methods [26] have mainly been used to tackle the nonconvexity in optimization problems from the oil and gas industry. Parallelization of these algorithms have been used to solve large scale problems [18]. Smoothing of discontinuities, which are usually present in many mechanical models, can improve the performance of these global optimization techniques [10], possibly with some degradation in solution accuracy.

However meta-heuristics have many drawbacks. First of all, they require a large number of the objective and constraint function evaluations which is not acceptable when their evaluations are expensive. This makes both simulated annealing and genetic algorithms suitable for only small problems. Second, meta-heuristics have difficulties in dealing with the complicated continuous constraint functions which are common for many optimization problems from the oil and gas industry. Third, meta-heuristics sometimes cannot locate a global solution with high accuracy: as a result they may produce only suboptimal solutions.

For large production system optimization problems, the preferred "standard" algorithms are still the Sequential Linear Programming (SLP) [13, 24] and Sequential Quadratic Programming (SQP) [9] methods. However, these methods also have their own limitations. In many integrated production system optimization involving gas blending such as in the liquified Natural Gas (LNG) processing, the simultaneous consideration of blending and fluid transmission can result in blending problems which are similar to the Haverly Pooling problem [14]. Problems of this type are generally nonconvex and can have multiple solutions [11]. In this situation, the local solvers may get stuck in one of the many stationary points.

Derivative free methods do not rely explicitly on the local model of the objective and/or constraint functions and therefore they are more effective to solve global and nonsmooth optimization than gradient or subgradient-based methods. In this paper we study the application of different versions of the derivative free Discrete Gradient Method (DGM) as well as the Lipschitz Global Optimizer (LGO) solver suite to production optimization in integrated oil and gas production systems and their comparison with various local and global solvers from the General Algebraic Modeling System (GAMS). It is well known that comparative studies of optimization algorithms can be problematic as there may be objections to the choice of parameters and procedures used (Dolan and Moré as cited in [17]). In this paper we analyze the performance of DGM and LGO applied to typical gas production optimization problems.

In integrated production system modeling and optimization, the coupling of subsurface dynamic reservoir models to surface network and processing plants models is non-trivial, with many tie-in possibilities [5]. In this paper, we follow earlier coupling ideas [25] but the minimum and maximum functions are used to combine the pressure/rate transmission equations and gas blending constraints into a single optimization problem. Four test problems, with increasing complexity in the objective and constraints functions are used to illustrate this approach. We present the results of numerical experiments on these test problems.

The paper is organized as follows. Section 2 describes optimization models in the integrated production systems. The description of optimization problems are given in Section 3. Section 4 gives the brief description of algorithms used in this paper and Section 5 presents the results of numerical experiments. We discuss the

results of numerical experiments and give some preliminary conclusions in Section 6.

2. **Mathematical model of the gas blending process.** We consider the process of the blending of gas produced from five fields $F_1, \ldots, F_5$ to supply different quality gas at six processing plants $P_1, \ldots, P_6$ through a converging-diverging gas gathering/distribution network, as shown in Figure 1.
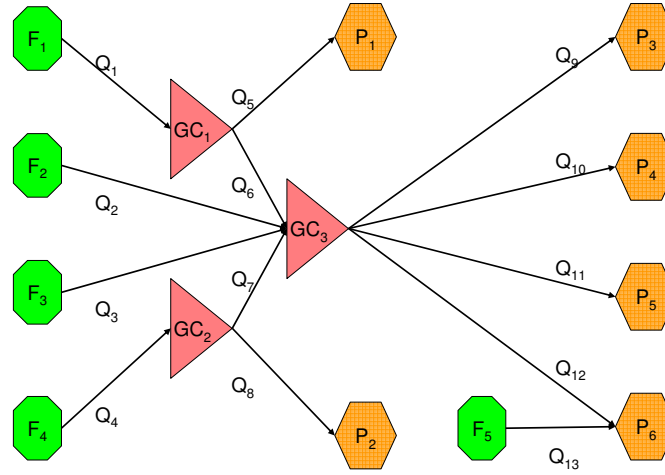

FIGURE 1. Scheme of the gas blending network

This model has five fields, where the average reservoir pressures are fixed and the relationship between the average reservoir pressure and flowing bottom hole pressure (FBHP) can be expressed as a quadratic Inflow Performance Relationship (IPR) (see, for example, [7]). From the bottom of the well to the tubing head, the Vertical Flow Performance (VFP), which associate the pressure drop in vertical pipes with production, is assumed to be quadratic.

In order to find flow rates $Q_1, ..., Q_{13}$ in the above gas network, a set of simultaneous equations is developed that relates the nodes' pressures with flow rates. The governing principles used for fluid flow in a network under steady state conditions are based on Kirchoff's law, and the fact that gas flows down a pressure gradient. It is assumed that flow controllers are present at the gathering centers GC_1, GC_2 and GC_3 to dissipate energy in order to equalize incoming pressures and spilt flow.

2.1. **Reservoir pressure.** The average reservoir pressures for the five fields $F_1, \ldots, F_5$ are, by assumption, fixed at 3569 psia (pound per square inch, absolute), 3688 psia, 3843 psia, 3935 psia and 4003 psia, respectively.

2.2. **Gas inflow performance relationship.** The determination of the flowing bottom hole pressure, P_{FBHP}, given the average reservoir pressure, P_{RES} and gas flow rate, Q, is based on the following Inflow Performance Relationship (IPR) equation:

$$P_{RES}^2 - P_{FBHP}^2 = A * Q + F * Q^2 \tag{1}$$

where A and F are Darcy and Non-Darcy flow coefficients, respectively. Like most IPR for gas-condensate reservoirs (see, [16] for other and newer IPRs), the dependence (1) is also quadratic. When the pressure is expressed in psia and gas flow rate expressed in MMscf/d (million standard cubic feet per day), the numerical values for flow coefficients of the five fields are shown in Table 1.

Field	A	F
F_1	1001009	6737
F_2	7738	52
F_3	194022	1305
F_4	9033	61
F_5	167005	1124

TABLE 1. Flow coefficients A and F .

2.3. **Gas vertical flow performance.** The vertical flow performance (VFP) for the wells is an adaptation of the Cullender-Smith equation [8]. The equation relates the flowing bottom flow pressure, P_{FBHP}, to the flowing tubing head pressure, P_{FTHP}, and the flow rate, Q, as follows:

$$P_{FBHP}^2 = B * P_{FTHP}^2 + C * Q^2. \tag{2}$$

The VFP flow coefficients for the five wells, for the same pressure and rate units as above, are shown in Table 2.

Field	B	C
F_1	1.85	1523
F_2	1.86	280
F_3	1.94	1767
F_4	1.98	337
F_5	2.07	2086

TABLE 2. VFP flow coefficients B and C.

2.4. **Well pressure-rate performance.** Equations (1) and (2) imply that the relationship of P_{THP} with Q for each field is given by

$$P_{THPi} = \frac{\sqrt{P_{RESi}^2 - A_i Q_i - (C_i + F_i)Q_i^2}}{\sqrt{B_i}}, \ i = 1, \ldots, 5. \tag{3}$$

2.5. **Pressure drop along horizontal pipes.** The pressure drop $(P_{IN} - P_{OUT})$ associated with a flow, Q, in a horizontal pipe is calculated from the equation:

$$P_{OUT} = \sqrt{P_{IN}^2 - H * Q^2}. \tag{4}$$

The coefficient H for each pipe in the network is shown in Figure 2. Like most pressure drop equations [12, 23], the above equation is also quadratic.

The minimum outlet pressures for $P_1, \ldots, P_6$ are 500 psia, 550 psia, 600 psia, 580 psia, 560 psia and 670 psia, respectively, as shown in Figure 3. The Tubing Head Pressure (THP) for all wells must be greater or equal to 1543 psia.
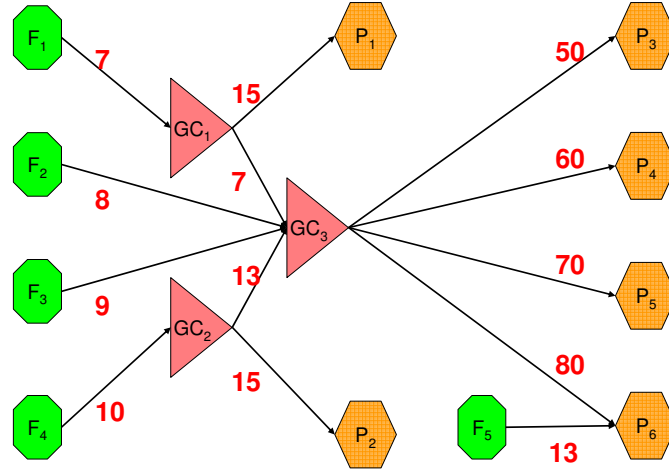
FIGURE 2. Pipe pressure drop coefficient H

2.6. **Network pressure-rate equations.** The THP provides the energy to drive the gas to deliver at or above the minimum delivery pressure at a plant. Some of the energy is lost due to friction. To illustrate the pressure-rate calculation, we will consider production from $F_1, \ldots, F_4$ to P_1 and P_3. The steps from F_1 to P_1, given Q_1, a decision variable, are illustrated below:

$$P_{THP1}^2 = \frac{P_{RES1}^2 - A_1 Q_1 - (C_1 + F_1)Q_1^2}{B_1}, \qquad (5)$$

$$P_{OUT1}^2 = P_{THP1}^2 - H_1 * Q_1^2, \qquad (6)$$

$$P_{OUT5}^2 = P_{OUT1}^2 - H_5 * Q_5^2. \qquad (7)$$

After substitution, P_{OUT5}^2 can be expressed as:

$$P_{OUT5}^2 = \frac{P_{RES1}^2 - A_1 Q_1 - (C_1 + F_1)Q_1^2}{B_1} - H_1 * Q_1^2 - H_5 * Q_5^2. \qquad (8)$$

For feasible flow, $P_{OUT5}^2 \geq (500psia)^2$, the squared of the minimum delivery pressure at P_1, therefore one condition for flow is:

$$\frac{P_{RES1}^2 - A_1 Q_1 - (C_1 + F_1)Q_1^2}{B_1} - H_1 * Q_1^2 - H_5 * Q_5^2 \geq 500^2. \qquad (9)$$

The condition for flow to the processing plant, P_3, is more involved as we have to consider production from F_1 to $F4$ and flow and blending at three gathering centers GC_1, GC_2 and GC_3.

The outlet pressures from the four fields at GC_3 are calculated as shown above and they are as follows:

$$P_{OUT6}^2 = \frac{P_{RES1}^2 - A_1 Q_1 - (C_1 + F_1)Q_1^2}{B_1} - H_1 * Q_1^2 - H_6 * Q_6^2, \qquad (10)$$

$$P_{OUT2}^2 = \frac{P_{RES2}^2 - A_2 Q_2 - (C_2 + F_2)Q_2^2}{B_2} - H_2 * Q_2^2, \tag{11}$$

$$P_{OUT3}^2 = \frac{P_{RES3}^2 - A_3 Q_3 - (C_3 + F_3)Q_3^2}{B_3} - H_3 * Q_3^2, \tag{12}$$

$$P_{OUT7}^2 = \frac{P_{RES4}^2 - A_4 Q_4 - (C_4 + F_4)Q_4^2}{B_4} - H_4 * Q_4^2 - H_7 * Q_7^2. \tag{13}$$

Then the pressure P_{GC3} at GC_3 is:

$$P_{GC3} = \min[P_{OUT6}, P_{OUT2}, P_{OUT3}, P_{OUT7}]. \tag{14}$$

Thus, the condition for flow from GC_3 to P_3 is as follows:

$$P_{GC3}^2 - H_9 * Q_9^2 \geq (600psia)^2 \tag{15}$$

or alternatively,

$$\min[P_{OUT6}^2, P_{OUT2}^2, P_{OUT3}^2, P_{OUT7}^2] - H_9 * Q_9^2 \geq (600psia)^2. \tag{16}$$

In addition to the above equations, at the gathering centers the following mole (and volume) conservation applies:

$$Q_1 - Q_5 - Q_6 = 0, \tag{17}$$

$$Q_4 - Q_7 - Q_8 = 0, \tag{18}$$

$$Q_2 + Q_3 + Q_6 + Q_7 - Q_9 - Q_{10} - Q_{11} - Q_{12} = 0. \tag{19}$$

2.7. **Gas composition.** It is desired that gas delivered to processing plant P_6 must meet CO_2 and N_2 concentration limits while maximizing LPG content. For the blending calculation, we need the gas composition of all the five fields as they all contribute towards production to P_6. The gas composition, in volume fraction, for the five fields are shown in Table 3.

Mole	F_1	F_2	F_3	F_4	F_5
N2	0.006663	0.021507	0.023881	0.013324	0.023273
CO2	0.095243	0.069502	0.025714	0.049802	0.054818
C1	0.797880	0.595579	0.695003	0.756350	0.676466
C2	0.049224	0.061650	0.070667	0.072361	0.059070
C3	0.018223	0.042565	0.046096	0.035477	0.035145
C4	0.008072	0.034419	0.028061	0.017898	0.027000
C5+	0.024695	0.174778	0.110578	0.054789	0.124228
Total	1.000000	1.000000	1.000000	1.000000	1.000000

TABLE 3. Field gas composition.

The concentrations of CO_2, N_2 and LPG at GC_3 are as follows:

$$[CO_2]_{GC3} = \frac{Q_6[CO_2]_{F_1} + Q_2[CO_2]_{F_2} + Q_3[CO_2]_{F_3} + Q_7[CO_2]_{F_4}}{Q_2 + Q_3 + Q_6 + Q_7}, \tag{20}$$

$$[N_2]_{GC3} = \frac{Q_6[N_2]_{F_1} + Q_2[N_2]_{F_2} + Q_3[N_2]_{F_3} + Q_7[N_2]_{F_4}}{Q_2 + Q_3 + Q_6 + Q_7}, \tag{21}$$

$$[LPG]_{GC_3} = \frac{Q_6[C_3 + C_4]_{F_1} + Q_2[C_3 + C_4]_{F_2} + Q_3[C_3 + C_4]_{F_3} + Q_7[C_3 + C_4]_{F_4}}{Q_2 + Q_3 + Q_6 + Q_7}.$$
(22)

Thus at P_6 we get

$$[CO_2]_{P_6} = \frac{Q_{12}[CO_2]_{GC_3} + Q_{13}[CO_2]_{F_5}}{Q_{12} + Q_{13}}$$
(23)

and likewise for $[N_2]_{P_6}$ and $[LPG]_{P_6}$.

3. **The optimization problems.** We will consider four different optimization problems. These problems may differ from each other by both objective and constraint functions. Their general form is as follows:

$$\text{maximize } f(Q) \text{ subject to } Q \in X \subset \mathbb{R}^{13}.$$
(24)

Here the function f may have one of the following forms:

1. The objective function for gas production

$$f_1(Q) = \sum_{i=1}^{4} Q_i + Q_{13};$$
(25)

2. The objective function for the amount of LPG produced at P_6:

$$f_2(Q) = \frac{Q_{12}\left(Q_6 LPG_{F_1} + Q_2 LPG_{F_2} + Q_3 LPG_{F_3} + Q_7 LPG_{F_4}\right)}{Q_2 + Q_3 + Q_6 + Q_7} + Q_{13} LPG_{F_5}$$
(26)

where $LPG_i = [C_3 + C_4]_i$ is the sum of the amount of the propane and butane components.

3. The objective function for maximization of LPG production at plant P_6 and total condensate production:

$$f_3(Q) = f_2(Q) + \sum_{i=1}^{4} 3Q_i[C_{5+}]_{F_i} + 3Q_{13}[C_{5+}]_{F_5}$$
(27)

In production operations the upper and lower bounds are generally known and here the decision variables Q_i, $i = 1, \ldots, 13$ are in the range between 0 MMscf/day and 200 MMscf/day.

The feasible set X is described by the following constraint functions. There are seven pressure/rate constraint equations to deliver as per minimum outlet pressure requirements shown in Figure 3:

$$\varphi_1(Q) \equiv \frac{P_{RES1}^2 - A_1 Q_1 - (C_1 + F_1)Q_1^2}{B_1} - H_1 * Q_1^2 - H_5 * Q_5^2 - (500psia)^2 \geq 0, \quad (28)$$

$$\varphi_2(Q) \equiv \frac{P_{RES4}^2 - A_4 Q_4 - (C_4 + F_4)Q_4^2}{B_4} - H_4 * Q_4^2 - H_8 * Q_8^2 - (550psia)^2 \geq 0, \quad (29)$$

$$\varphi_3(Q) \equiv \min[P_{OUT6}^2, P_{OUT2}^2, P_{OUT3}^2, P_{OUT7}^2] - H_9 * Q_9^2 - (600psia)^2 \geq 0, \quad (30)$$

$$\varphi_4(Q) \equiv \min[P_{OUT6}^2, P_{OUT2}^2, P_{OUT3}^2, P_{OUT7}^2] - H_{10} * Q_{10}^2 - (580psia)^2 \geq 0, \quad (31)$$

$$\varphi_5(Q) \equiv \min[P^2_{OUT6}, P^2_{OUT2}, P^2_{OUT3}, P^2_{OUT7}] - H_{11} * Q^2_{11} - (560psia)^2 \geq 0, \quad (32)$$

$$\varphi_6(Q) \equiv \min[P^2_{OUT6}, P^2_{OUT2}, P^2_{OUT3}, P^2_{OUT7}] - H_{12} * Q^2_{12} - (670psia)^2 \geq 0, \quad (33)$$

$$\varphi_7(Q) \equiv \frac{P^2_{RES5} - A_5 Q_{13} - (C_5 + F_5)Q^2_{13}}{B_5} - H_{13} * Q^2_{13} - (670psia)^2 \geq 0. \quad (34)$$

There are three volume (mole) fraction constraints for CO_2 and N_2 at GC_3 and LPG_{P_5}:

$$\varphi_8(Q) \equiv [CO_2]_{GC_3} - 0.05 \leq 0, \quad (35)$$

$$\varphi_9(Q) \equiv [N_2]_{GC_3} - 0.03 \leq 0, \quad (36)$$

$$\varphi_{10}(Q) \equiv \frac{Q_{12}(Q_{12} + Q_{13})(Q_6 LPG_{F_1} + Q_2 LPG_{F_2} + Q_3 LPG_{F_3} + Q_7 LPG_{F_4})}{Q_2 + Q_3 + Q_6 + Q_7}$$
$$+ \frac{Q_{13} LPG_{F_5}}{Q_{12} + Q_{13}} - 0.06 \geq 0. \quad (37)$$

In addition there are three linear equalities from (17) - (19) describing mole (and volume) conservation at the gathering centers:

$$\varphi_{11}(Q) = Q_1 - Q_5 - Q_6 = 0, \quad (38)$$

$$\varphi_{12}(Q) = Q_4 - Q_7 - Q_8 = 0, \quad (39)$$

$$\varphi_{13}(Q) = Q_2 + Q_3 + Q_6 + Q_7 - Q_9 - Q_{10} - Q_{11} - Q_{12} = 0. \quad (40)$$

It should be noted that functions $\varphi_1, \ldots, \varphi_7$ are concave, φ_8, φ_9 are nonconvex and φ_{10} is nonconcave.

We will consider the following problems.

Problem 1. maximize $f_1(Q)$ ubject to $x \in X_1 = \{Q \in \mathbb{R}^{13} : 0 \leq Q_i \leq 200, \ i = 1, \ldots, 13, \ \varphi_i(Q) = 0, \ i = 11, 12, 13, \ \varphi_i(Q) \geq 0, \ i = 1, \ldots, 7\}$.

Since f_1 is linear function and the set X_1 is convex the problem (1) is convex.

Problem 2. maximize $f_1(Q)$ subject to $x \in X_2 = \{Q \in \mathbb{R}^{13} : 0 \leq Q_i \leq 200, \ i = 1, \ldots, 13, \ \varphi_i(Q) = 0, \ i = 11, 12, 13, \ \varphi_i(Q) \geq 0, \ i = 1, \ldots, 10\}$.

Despite the fact that f_1 is linear function, the set X_2 is nonconvex and therefore the problem (2) is nonconvex and it may have many local minimizers.

Problem 3. maximize $f_2(Q)$ subject to $x \in X_2$.

In this problem both the objective function and the feasible set X_2 are nonconvex and therefore the problem (3) is nonconvex.

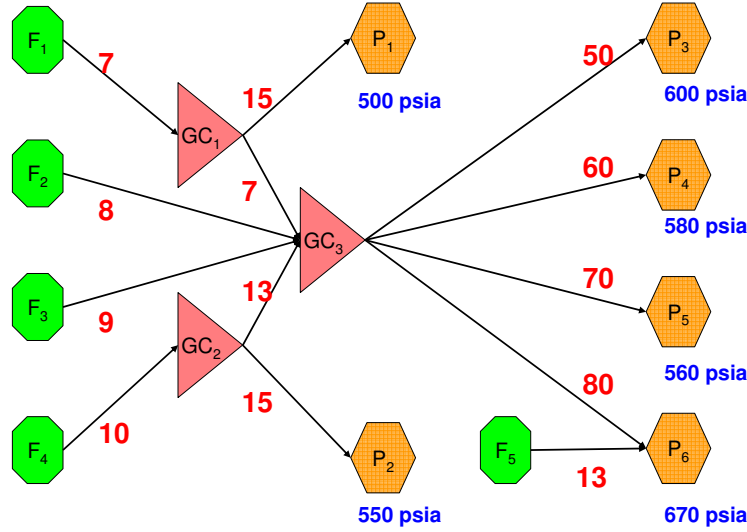**Problem 4.** maximize $f_3(Q)$ subject to $x \in X_2$.

The problem (4) is nonconvex.

FIGURE 3. Minimum Outlet Delivery Pressure Requirements (in psia)

4. Optimization algorithms.

4.1. **Discrete gradient method.** The discrete gradient method (DGM) was introduced and studied for different nonsmooth optimization problems in [1, 2, 3, 4]. Here we use four different versions of DGM. Their main difference is the way they compute descent directions. Therefore we will describe here only an algorithm for the computation of descent directions in DGM. The description of DGM itself can be found in the above mentioned papers.

Let f be a locally Lipschitz continuous function defined on $\mathbb{R}^n$. Let

$$S_1 = \{g \in \mathbb{R}^n : \|g\| = 1\}, \ G = \{e \in \mathbb{R}^n : e = (e_1, \ldots, e_n), |e_j| = 1, \ j = 1, \ldots, n\},$$

$$P = \{z(\lambda) : z(\lambda) \in \mathbb{R}^1, \ z(\lambda) > 0, \ \lambda > 0, \ \lambda^{-1}z(\lambda) \to 0, \ \lambda \to 0\}.$$

Here S_1 is the unit sphere, G is the set of vertices of the unit hypercube in $\mathbb{R}^n$ and P is the set of univariate positive infinitesimal functions.

We take any $g \in S_1$ and define $|g_i| = \max\{|g_k|, \ k = 1, \ldots, n\}$. We also take any $e = (e_1, \ldots, e_n) \in G$, a positive number $\alpha \in (0, 1)$ and define the sequence of n vectors $e^j(\alpha), \ j = 1, \ldots, n$:

$$
\begin{aligned}
e^1(\alpha) &= (\alpha e_1, 0, \ldots, 0), \\
e^2(\alpha) &= (\alpha e_1, \alpha^2 e_2, 0, \ldots, 0), \\
\ldots &= \ldots\ldots\ldots \\
e^n(\alpha) &= (\alpha e_1, \alpha^2 e_2, \ldots, \alpha^n e_n).
\end{aligned}
$$

Then for given $x \in \mathbb{R}^n$ and $z \in P$ we define a sequence of $n+1$ points as follows:

$$
\begin{aligned}
x^0 &= x + \lambda g, \\
x^1 &= x^0 + z(\lambda)e^1(\alpha), \\
x^2 &= x^0 + z(\lambda)e^2(\alpha), \\
\ldots &= \ldots \quad \ldots \\
x^n &= x^0 + z(\lambda)e^n(\alpha).
\end{aligned}
$$

Definition 1. (see [1] - [4]) The discrete gradient of the function f at the point $x \in \mathbb{R}^n$ is the vector $\Gamma^i(x, g, e, z, \lambda, \alpha) = (\Gamma_1^i, \ldots, \Gamma_n^i) \in \mathbb{R}^n, g \in S_1$ with the following coordinates:

$$\Gamma_j^i = [z(\lambda)\alpha^j e_j)]^{-1} \left[f(x^j) - f(x^{j-1}) \right], \; j = 1, \ldots, n, \; j \neq i,$$

$$\Gamma_i^i = (\lambda g_i)^{-1} \left[f(x^n) - f(x) - \sum_{j=1, j\neq i}^{n} \Gamma_j^i \left(\lambda g_j - z(\lambda)\alpha^j e_j \right) \right].$$

Remark 1. One can see from the definition that $n - 1$ coordinates of the discrete gradient are computed differently from its i-th coordinate. They are approximations to $n-1$ coordinates of a certain subgradient at the point $x + \lambda g$ and these coordinates dependent in particular on $z \in P$. One can take z very small number and fix it for all $\lambda > 0$ or $z \in P$ can be any univariate positive infinitesimal function. Discrete gradients approximate subgradients for a broad subset of nonsmooth functions [3, 4].

Let $z \in P, \lambda > 0, \alpha \in (0, 1]$, the number $c \in (0, 1)$ and a tolerance $\delta > 0$ be given.

Algorithm 1. An algorithm for the computation of the descent direction.

Step 1. Choose any $g^1 \in S_1, e \in G$, compute $i = \text{argmax}\{|g_j|, \; j = 1, \ldots, n\}$ and a discrete gradient $v^1 = \Gamma^i(x, g^1, e, z, \lambda, \alpha)$. Set $\overline{D}_1(x) = \{v^1\}$ and $k = 1$.

Step 2. Calculate the vector $\|w^k\|^2 = \min\{\|w\|^2 : w \in \overline{D}_k(x)\}$. If

$$\|w^k\| \leq \delta, \tag{41}$$

then stop. Otherwise go to Step 3.

Step 3. Calculate the search direction by $g^{k+1} = -\|w^k\|^{-1} w^k$.
Step 4. If

$$f(x + \lambda g^{k+1}) - f(x) \leq -c\lambda\|w^k\|, \tag{42}$$

then stop. Otherwise go to Step 5.

Step 5. Compute $i = \text{argmax}\{|g_j^{k+1}| : \; j = 1, \ldots, n\}$ and a discrete gradient

$$v^{k+1} = \Gamma^i(x, g^{k+1}, e, z, \lambda, \alpha),$$

construct the set $\overline{D}_{k+1}(x) = \text{co}\{\overline{D}_k(x) \bigcup\{v^{k+1}\}\}$, set $k = k + 1$ and go to Step 2.

Remark 2. Algorithm 1 is a terminating [3, 4]. This fact is true for any values of $\lambda > 0$. Small values of $\lambda > 0$ give approximations to subgradients of f and in this case Algorithm 1 calculates local descent directions. Large values of $\lambda > 0$ do not give approximations to subgradients anymore however they still allow one to find descent directions from x and such directions are global descent directions. Algorithm 1 is capable of finding such directions even from local minimizers.

We will consider four different versions of the discrete gradient method: DGM1L, DGM1G, DGM2L and DGM2G. In DGM1L and DGM1G discrete gradients are computed using $z(\lambda) = \lambda^l$ where $l \geq 2$ whereas $z(\lambda) = 10^{-12}$ for any $\lambda > 0$ in DGM2L and DGM2G. Only local descent directions are computed in DGM1L and DGM2L. In DGM1G and DGM2G both local and global descent directions are computed.

The idea behind both DGM1G and DGM2G is the same. We take any starting point and applying DGM1L (or DGM2L in DGM2G) compute the first local solution. Then applying the algorithm for the computation of global descent directions we find descent direction from this local minimizer and compute a new starting point for DGM1L (or DGM2L) and so on. This continues until the algorithm for the computation of global descent directions cannot find a descent direction from a local minimizer.

4.2. **The Lipschitz-continuous global optimizer.** The Lipschitz-Continuous Global Optimizer (LGO) solver suite has been successfully applied to complex, large-scale models both in research and commercial contexts for over a decade. Detailed technical descriptions and user documentation can be found in [19] and [20] and elsewhere, including the peer review [6]. LGO solver suites is based on a seamless combination of a suite of global and local scope nonlinear solvers. Currently, LGO includes the following solver options:

- Branch-and-bound (adaptive partition and sampling) based global search (LGO-BB);
- Adaptive global random search (with single-start) (LGO-GARS);
- Adaptive multi-start global random search (LGO-MS).
- Constrained local search based on the generalized reduced gradient method (GRG) (LGO-LS).

The LGO global search methodology has been described in [19], [20] and Section 2 of [21] reviews several implementations. In all three global search modes the model functions are aggregated by an exact penalty (aggregated merit) function. By contrast, in the local search phase all model functions are considered and treated individually. The global search phases are equipped also with stochastic sampling procedures that support the usage of statistical bound estimation methods. All LGO search algorithms are derivative-free: specifically, in the local search phase central differences are used to approximate gradients. The compiler-based LGO solver suite is used as an option linked to various modeling environments [21]. In its core text I/O based version, the application-specific LGO executable program (that includes a driver file, the LGO solver library and the model function file) reads an input text file that contains application-specific information (model name, variable and constraint names, variable bounds and nominal values, and constraint types) as well as a few key solver options (global solver type, precision settings, resource and time limits). Upon completing the LGO run, a summary and a detailed report file are available. As can be expected, this LGO version has the lowest demands for hardware, it also is fastest and can be directly embedded into vertical and proprietary user applications.

4.3. **GAMS local and global solvers.** For an independent verification and comparison, the four test problems were run through various local and global solvers available in GAMS. Brief descriptions of the solvers are as follows (see http://www.gams.com/solvers/solvers.htm, for more details):

- SNOPT is a large scale Sequential Quadratic Programming (SQP) solver developed by Philip Gill (University of California at San Diego) and Walter Murray and Michael Saunders (Stanford University).
- MINOS from the Systems Optimization Laboratory at Stanford University iteratively solves subproblems with linearized constraints and an augmented Lagrangian objective function. MSMINOS is MINOS with multi-start.

- KNITRO from Ziena Optimization, Inc is a software package for finding local solutions of continuous, smooth nonlinear optimization problems, with or without constraints.
- PATHNLP solves an NLP by internally constructing the Karush-Kuhn-Tucker (KKT) system of first-order optimality conditions associated with the NLP and solving this system using the PATH solver for complementarity problems.
- CONOPT from ARKI Consulting and Development in Denmark is a generalized reduced gradient solver. MSCONOPT is multi-start CONOPT.
- OQNLP, from Optimal Methods and OptTek Systems, Inc., is a solver for global optimization of smooth constrained problems with either all continuous variables or a mixture of discrete and continuous variables.
- MSNLP (Multi-Start NLP) is another stochastic search algorithm from Optimal Methods, Inc. for global optimization problems.
- OQCONOPT combines the OptQuest (OQ) Callable Library (a scatter search code) of Glover, Laguna, Kelly with the CONOPT solver.
- OQMINOS combines the OQ Callable Library with MINOS.

5. **Results of numerical experiments.** It is obvious from the construction that the above formulated optimization problems can have multiple solutions, which is what we expect in real world production operations. In production operations the upper and lower bounds are generally known and for the test cases, the decision variables are in the range between 0 MMscf/day and 200 MMscf/day. The starting point for each variable is set to the mid-point value of 100 MMscf/day. However, this selection may be an infeasible starting point which it is in these test cases.

LGO is available for the Mathematica (version 5.1 was used) platform as the MathOptimizer Professional (MOP) software package. MOP auto-converts the Mathematica model code into Fortran (the compiler used was Intel Fortran version 7.1) and then the external LGO engine solves the model. Results are reported back to the calling Mathematica document (see [22]).

No tuning of search parameters was made for the algorithms and all were run in the default option mode. All versions of DGM have no user tuneable parameters which is an important feature for deployment in the operating companies.

5.1. **Problem 1: maximizing gas production.** The solutions obtained by LGO and DGM are shown in Table 4.

One can see from Table 4 that the LGO-GARS and LGO-MS solutions are better than those obtained by the different versions of DGM. However, the DGM results are better than LGO-BBLS and LGO-LS (recall that the latter is only a local solver mode usage of LGO).

The solutions by LGO-GARS, LGO-MS, LGO-LS and LGO-BB were obtained with the maximum constraint violation of $5 \times 10^{-6}, 5 \times 10^{-6}, 7 \times 10^{-7}$ and 7×10^{-7}, respectively. The solutions of the DGM variants were obtained to the maximum constraint violation of less than 10^{-10}. This may explain why the LGO-GARS and LGO-MS results were slightly better albeit with acceptable constraint violation. For engineering purposes, all these solutions are acceptable.

The solutions obtained by local and global solvers of GAMS, with constraint violation of about 10^{-6} are shown in Tables 5 and 6. SNOPT and MINOS failed to come up with feasible solution and the OQMINOS solution was suboptimal. From the various solutions, with almost similar values of the objective function,

Variable	LGO-GARS	LGO-MS	LGO-LS	LGO-BB	DGM1L	DGM1G	DGM2L	DGM2G
Q_1	7.820	7.820	0.000	0.000	7.820	7.820	7.820	7.818
Q_2	154.975	154.975	154.975	154.975	133.816	114.016	140.110	151.503
Q_3	34.005	34.005	0.000	0.000	33.147	33.731	26.259	32.050
Q_4	153.579	153.579	153.579	153.579	151.767	147.552	150.886	153.579
Q_5	2.250	0.000	0.000	0.000	3.530	5.909	4.647	7.218
Q_6	5.570	7.820	0.000	0.000	4.291	1.911	3.173	0.600
Q_7	126.110	0.000	131.622	131.622	6.870	91.526	136.405	115.092
Q_8	27.470	153.579	21.957	21.957	144.897	56.026	14.481	38.487
Q_9	23.999	59.920	47.529	47.529	8.597	66.293	143.995	10.604
Q_{10}	70.708	13.224	77.826	77.826	157.303	65.977	11.853	139.561
Q_{11}	131.697	53.171	54.863	54.863	9.860	65.661	136.765	12.552
Q_{12}	94.256	70.485	106.380	106.380	2.365	43.252	13.333	136.528
Q_{13}	38.277	38.277	38.277	38.277	10.734	34.595	29.842	14.035
Value	388.657	388.657	346.832	346.832	337.285	337.715	354.917	358.985

TABLE 4. LGO and DGM solutions for Problem 1

this problem has multiple solutions. The consensus optimal value in the objective function is 388.657 with the maximum constraint violation of less than 10^{-6}.

Variable	KNITRO	PATHNLP	CONOPT	MSCONOPT	MSMINOS
Q_1	7.820	7.820	7.820	7.820	7.820
Q_2	154.975	154.975	154.975	154.975	154.975
Q_3	34.005	34.005	34.005	34.005	34.005
Q_4	153.579	153.579	153.579	153.579	153.579
Q_5	3.846	5.694	0.000	0.000	0.149
Q_6	3.974	2.126	7.820	7.820	7.671
Q_7	80.572	118.746	0.000	0.000	9.517
Q_8	73.007	34.833	153.579	153.579	144.063
Q_9	71.355	96.810	149.955	149.955	0.000
Q_{10}	69.464	83.207	46.845	46.845	91.833
Q_{11}	67.771	72.676	0.000	0.000	39.221
Q_{12}	64.936	57.159	0.000	0.000	75.113
Q_{13}	38.277	38.277	38.277	38.277	38.277
Value	388.657	388.657	388.657	388.657	388.657

TABLE 5. Solutions from various GAMS local solvers with both single start and multi-start options for Problem 1.

5.2. **Problem 2: maximizing gas production with gas quality constraints.** The solutions obtained by LGO solvers and different versions of DGM are presented in Table 7.

The solutions by the various local and global solvers of GAMS are presented in Tables 8 and 9. The solvers SNOPT, MINOS, KNITRO and PATHNLP failed to locate any feasible solution. However, the multi-start MINOS managed to converge to a feasible solution but no such improvement was observed for CONOPT (see Table 8).

From the results of the various GAMS and the LGO solvers, the consensus best value for the objective function is 276.6. DGM1L and DGM1G search modes did come up with better values but these were achieved at the expense of a single constraint violation (Equation 35) in the order of 10^{-2}. The maximum constraint

Variable	OQNLP	MSNLP	OQCONOPT	OQMINOS
Q_1	7.820	7.820	7.820	7.707
Q_2	154.975	154.975	154.975	54.521
Q_3	34.005	34.005	34.005	8.886
Q_4	153.579	153.579	153.579	32.188
Q_5	0.000	0.000	0.000	7.707
Q_6	7.820	7.820	7.820	0.000
Q_7	108.911	108.911	0.000	16.911
Q_8	44.668	44.668	153.579	15.277
Q_9	78.377	78.377	149.955	17.976
Q_{10}	78.302	78.302	46.845	35.843
Q_{11}	78.227	78.227	0.000	13.657
Q_{12}	70.804	70.804	0.000	12.841
Q_{13}	38.277	38.277	38.277	7.642
Value	388.657	388.657	388.657	110.943

TABLE 6. Solutions obtained by GAMS global solvers for Problem 1.

Variable	LGO-CARS	LGO-MS	LGO-LS	LGO-BB	DGM1L	DGM1G	DGM2L	DGM2G
Q_1	7.820	7.820	0.000	0.000	7.820	7.820	6.156	6.156
Q_2	42.955	42.955	42.642	42.642	137.162	137.162	111.777	111.777
Q_3	34.005	34.005	34.005	34.005	33.970	33.970	23.991	23.991
Q_4	153.579	153.579	153.579	153.579	153.579	153.579	135.929	135.929
Q_5	7.820	7.820	0.000	0.000	7.729	7.729	6.156	6.156
Q_6	0.000	0.000	0.000	0.000	0.091	0.091	0.000	0.000
Q_7	153.579	153.579	99.974	99.974	93.261	93.261	105.846	105.846
Q_8	0.000	0.000	53.606	53.606	60.319	60.319	30.083	30.083
Q_9	23.999	8.371	75.147	75.147	73.048	73.048	18.638	18.638
Q_{10}	70.708	49.717	51.549	51.549	72.776	72.776	72.501	72.501
Q_{11}	56.454	61.831	40.465	40.465	72.505	72.505	75.328	75.328
Q_{12}	79.377	110.619	9.460	9.460	46.155	46.155	75.147	75.147
Q_{13}	38.277	38.277	38.277	38.277	32.190	32.190	38.277	38.277
Value	276.636	276.636	268.503	268.503	364.722	364.722	316.130	316.130

TABLE 7. LGO and DGM solutions for Problem 2.

violation for the other three LGO and GAMS solvers is about 10^{-6}. This may explain why the DGM solutions are better.

5.3. **Problem 3: plant P_6 LPG maximization.** Results for LGO solvers and different versions of DGM are presented in Table 10.

One can see from Table 10 that In this test case, LGO gave better solutions compared to the two DGM versions. For the first three LGO solutions the constraint violations were all less than $1.1 \cdot 10^{-7}$. The constraint violation for the LGO-BB was $4.5 \cdot 10^{-6}$. It is intuitive that for this test case the best strategy would be to divert as much gas to Plant P_6 as possible. This is indeed the case for the three LGO algorithms.

Results for GAMS solvers are shown in Tables 11 and 12 and these results show that Problem 3 has many solutions and different solvers given the same starting point, which is the mid-point of the lower and upper bounds. Overall, MSCONOPT (multi-start CONOPT) gave the best solution, followed by LGO-MS. MINOS, MSMINOS and SNOPT failed to locate feasible solutions.

Variable	CONOPT	MSCONOPT	MSMINOS
Q_1	7.820	7.820	7.820
Q_2	42.955	42.955	42.801
Q_3	34.005	34.005	34.005
Q_4	153.579	153.579	153.579
Q_5	7.820	7.820	7.820
Q_6	0.000	0.000	0.000
Q_7	153.579	153.579	127.214
Q_8	171.951	0.000	26.365
Q_9	17.766	171.951	4.591
Q_{10}	17.766	17.766	50.864
Q_{11}	23.056	17.766	92.142
Q_{12}	38.277	23.056	56.423
Q_{13}	0.000	38.277	38.277
Value	276.636	276.636	276.482

TABLE 8. Solutions from various GAMS local solvers with both single start and multi-start options for Problem 2.

Variable	OQNLP	MSNLP	OQCONOPT	OQMINOS
Q_1	7.820	7.820	7.820	7.820
Q_2	42.955	42.963	42.955	42.838
Q_3	34.005	34.005	34.005	34.005
Q_4	153.579	153.579	153.579	153.579
Q_5	7.820	7.820	7.820	7.820
Q_6	0.000	0.000	0.000	0.000
Q_7	153.579	153.579	153.579	133.508
Q_8	0.000	0.000	0.000	20.071
Q_9	114.495	0.000	171.951	60.795
Q_{10}	23.716	0.000	17.766	58.021
Q_{11}	46.674	147.588	17.766	47.791
Q_{12}	45.653	82.959	23.056	43.745
Q_{13}	38.277	38.277	38.277	38.277
Value	276.636	276.645	276.636	276.519

TABLE 9. Solutions obtained by GAMS global solvers for Problem 2.

5.4. Problem 4: plant P_6 LPG and total condensate production maximization.

The solutions are as shown in Table 13.

For this problem case, the DGM gave better solutions than the LGO. The DGM solution were some 50% better.

The solutions obtained by GAMS solvers are shown in Tables 14 and 15.

One can see that Problem 4 has multiple solutions and different solvers produce different solutions starting from the the same point. Overall, DGM gave the best solutions. SNOPT, MINOS and MSMINOS failed to locate feasible solutions.

6. Discussions and conclusions.

"The future is gas", said Jeroen van der Veer, the Chief Executive of the Royal Dutch Shell plc, in a speech delivered on the 23rd World Gas Conference held in Amsterdam on June 6, 2006. It is anticipated that over the next two decades, gas either transported in pipelines or as Liquified Natural Gas (LNG) will be the major business of many major oil and gas companies. Optimization algorithms may play important role to meet the challenges of gas

Variable	LGO-GARS	LGO-MS	LGO-LS	LGO-BB	DGM1L	DGM1G	DGM2L	DGM2G
Q_1	0.000	0.000	0.000	6.941	2.000	2.001	7.226	2.000
Q_2	42.911	36.028	42.517	39.375	40.203	35.670	154.917	113.643
Q_3	34.005	28.518	34.005	31.340	12.914	20.220	29.386	32.058
Q_4	146.159	129.639	145.900	139.786	8.738	9.784	152.242	5.000
Q_5	0.000	0.000	0.000	6.941	2.000	2.000	7.226	2.000
Q_6	0.000	0.000	0.000	0.000	0.000	0.001	0.000	0.000
Q_7	146.159	129.639	78.460	104.831	3.738	4.784	49.762	0.000
Q_8	0.000	0.000	67.440	34.955	5.000	5.000	102.481	5.000
Q_9	0.000	0.000	0.000	0.000	4.819	3.213	10.382	0.000
Q_{10}	34.467	0.000	0.000	0.000	5.820	4.138	96.438	0.303
Q_{11}	33.630	0.000	0.000	0.000	6.823	5.168	41.727	1.483
Q_{12}	154.978	194.185	154.982	175.546	39.394	48.156	85.518	143.914
Q_{13}	38.277	37.678	38.277	37.590	38.277	38.277	21.713	36.314
Value	11.863	14.171	12.378	13.306	5.330	5.956	7.483	13.262

TABLE 10. LGO and DGM solutions for Problem 3.

Variable	KNITRO	PATHNLP	CONOPT	MSCONOPT	MSMINOS
Q_1	7.820	7.820	7.820	0.433	25.908
Q_2	42.448	42.448	42.448	36.027	43.864
Q_3	34.005	34.005	34.005	28.517	48.363
Q_4	153.579	153.579	153.579	129.645	154.508
Q_5	7.820	7.820	7.820	0.433	25.908
Q_6	0.000	0.000	0.000	0.000	0.000
Q_7	66.653	66.653	66.653	129.645	154.508
Q_8	86.926	86.926	86.926	86.926	0.000
Q_9	0.000	0.000	0.000	0.000	0.000
Q_{10}	0.000	0.000	0.000	0.000	0.000
Q_{11}	0.000	0.000	0.000	0.000	125.400
Q_{12}	143.105	143.105	143.105	194.190	121.335
Q_{13}	38.277	38.277	38.277	38.277	44.837
Value	13.604	6.876	12.378	14.208	11.741

TABLE 11. Solutions from various GAMS local solvers with both
single start and multi-start options for Problem 3.

production and blending systems. Most of optimization problems in these systems
are nonconvex and nonsmooth global optimization problems.

It is well known that gas optimization problems, as typified by the Haverly gas
pooling problem [14], are nonconvex and can have multiple solutions [11]. Pro-
duction behaviors in nature may have many discontinuities and so are generally
nonsmooth and nonconvex. Therefore, depending on starting points, one of the lo-
cal scope solvers (such as SLP and SQP) may end up at a local minimizer. Finding
the best among the many local optima may lead to substantial business advan-
tages. On the other hand, data from gas production systems may contain noise
which makes the application of gradient-based methods impossible to solve in such
problems. Since the derivative-free methods do not rely explicitly on the local
models of the objective and/or constraint functions such methods are suitable for
solving many gas blending optimization problems. In this paper we pursue the use
of derivative-free techniques such as the LGO and the DGM.

In gas production optimization with blending, it is desirable to be able to take
into account the flow splitting and pressure dissipation in gathering and distribution

Variable	OQNLP	MSNLP	OQCONOPT	OQMINOS
Q_1	7.820	7.820	7.820	0.000
Q_2	42.460	42.460	36.027	42.460
Q_3	33.957	33.957	28.517	33.957
Q_4	78.966	78.966	129.645	84.400
Q_5	7.820	7.820	7.820	0.000
Q_6	0.000	0.000	0.000	0.000
Q_7	78.966	78.966	129.645	78.966
Q_8	0.000	0.000	0.000	0.000
Q_9	0.000	0.000	0.000	0.000
Q_{10}	0.000	0.000	0.000	0.000
Q_{11}	0.000	0.000	0.000	0.000
Q_{12}	155.383	155.383	194.190	155.383
Q_{13}	38.277	38.277	38.277	31.131
Value	12.397	12.397	14.208	11.953

TABLE 12. Solutions obtained by GAMS global solvers for Problem 3.

Variable	LGO-GARS	LGO-MS	LGO-LS	LGO-BB	DGM1L	DGM1G	DGM2L	DGM2G
Q_1	0.588	7.820	0.000	0.000	4.370	1.661	7.385	5.498
Q_2	42.942	42.448	42.752	42.752	135.601	154.975	154.973	154.935
Q_3	34.005	34.005	34.005	34.005	32.377	31.351	30.780	30.203
Q_4	153.579	153.579	153.579	153.579	145.956	130.373	146.169	132.373
Q_5	0.588	7.820	0.000	0.000	1.646	1.660	7.385	5.498
Q_6	0.000	0.000	0.000	0.000	2.724	0.001	0.000	0.000
Q_7	151.443	66.653	118.869	118.790	88.552	57.750	83.574	90.655
Q_8	2.136	86.926	34.710	34.789	57.404	72.623	62.595	41.718
Q_9	23.790	0.000	0.000	0.000	70.669	79.475	10.894	74.834
Q_{10}	70.499	0.000	34.607	34.562	70.352	65.894	72.240	73.155
Q_{11}	56.246	0.000	23.523	23.478	70.036	60.708	130.116	51.467
Q_{12}	77.854	143.105	137.495	137.506	48.197	38.000	56.077	76.337
Q_{13}	36.486	38.277	38.277	38.277	38.277	26.083	10.272	33.418
Value	79.680	85.347	84.125	84.126	126.038	127.204	124.350	133.171

TABLE 13. LGO and DGM Solutions for Problem 4.

networks, as shown in Figure 1. We took advantage of the capability of the DGM and LGO to solve nonsmooth problems and introduced the use of the minimum function to model chokes and flow controllers in production systems. In the forward flow from the well to the processing plant, termed the "forward-pass", the condition of flow at any gathering center, is that the operating pressure there is the minimum of the inlet pressures feeding into the gathering center. Excess pressures of the other inlets at the gathering center are dissipated through chokes and valves. In the "backward-pass", given the minimum delivery pressures at the plant, the maximum function is used to cascade the pressures and rates back to the production wells. This approach allows us to incorporate the network pressure/flow rate constraints and the blending requirements into a single optimization problem.

The above test problems model real-world situations. In this study, we are interested in the range of engineering solutions rather than just the performance of individual algorithms. Starting from a simple gas optimization under pressure constraints we gradually add blending requirements which involve fractional terms into the constraints and objective functions. The CO_2 volume fraction constraint (35)

Variable	KNITRO	PATHNLP	CONOPT	MSCONOPT	MSMINOS
Q_1	7.820	7.820	7.820	7.820	7.820
Q_2	42.448	42.448	42.448	42.448	42.448
Q_3	34.005	34.005	34.005	34.005	34.005
Q_4	153.579	153.579	153.579	153.579	153.579
Q_5	7.820	7.820	7.820	7.820	7.820
Q_6	0.000	0.000	0.000	0.000	0.000
Q_7	66.653	66.653	66.653	66.653	66.653
Q_8	86.926	86.926	86.926	86.926	86.926
Q_9	0.000	0.000	0.000	0.000	0.000
Q_{10}	0.000	0.000	0.000	0.000	0.000
Q_{11}	0.000	0.000	0.000	0.000	0.000
Q_{12}	143.105	143.105	143.105	143.105	143.105
Q_{13}	38.277	38.277	38.277	38.277	38.277
Value	85.347	85.347	85.347	85.347	85.347

TABLE 14. Solutions from various GAMS local solvers for Problem 4.

Variable	OQNLP	MSNLP	OQCONOPT	OQMINOS
Q_1	0.672	0.687	7.820	7.820
Q_2	7.820	7.820	42.448	42.257
Q_3	42.448	42.448	34.005	34.005
Q_4	34.005	34.005	153.579	153.579
Q_5	153.579	153.579	7.820	7.820
Q_6	7.820	7.820	0.000	0.000
Q_7	0.000	0.000	66.653	33.948
Q_8	66.653	66.653	86.926	119.631
Q_9	86.926	86.926	0.000	0.000
Q_{10}	0.000	0.000	0.000	57.523
Q_{11}	0.000	0.000	0.000	0.000
Q_{12}	0.000	0.000	143.105	52.687
Q_{13}	143.105	143.105	38.277	38.277
Value	85.347	85.347	85.347	79.518

TABLE 15. Solutions generated by GAMS global solvers for Problem 4.

presents considerable challenge for DGM. Although DGM came up with the best value at 368.33 (Table 7), it did so while violating the constraint (35) in the order of 0.007. From the results of the various GAMS and the LGO solvers, the consensus best value for the objective function of Problem 2 is 276.6. When the constraint (35) is expressed as a polynomial function instead of a fraction, both DGM1G and DGM2G gave an objective function value of 250.84 with no constraint violations ($< 10^{-8}$). So DGM1G and DGM2G are both capable algorithm. From an engineering perspective, the valid GAMS and LGO solutions where the objective function values are close to 276.6 are also acceptable.

In Problem 3, we introduced a fractional objective function, to test the capability of the DGM to address cases where blending is part of the objective function as well; in this case the maximization of LPG production at a particular plant. As shown in Table 10, only DGM2G came close to those obtained by LGO. For the GAM solvers, there is a wide spread in feasible solutions, ranging from 6.9 to 14.21, indicating that this problem has multiple solutions. As in Problem 2, when the constraint (35) is expressed as a polynomial function, DGM2G gave an objective
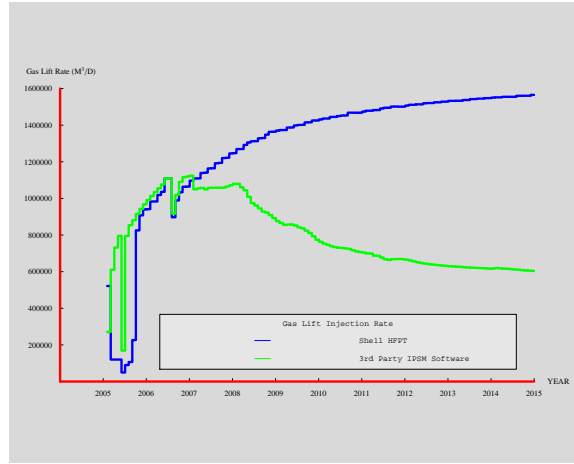
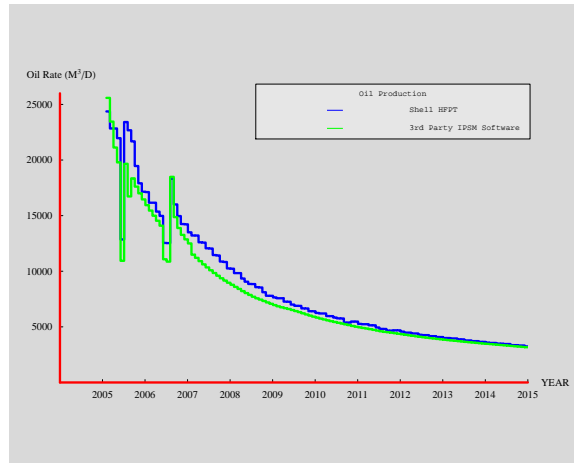FIGURE 4. Compared to a 3rd party package, HFPT/LGO gave better gas lift allocation.

FIGURE 5. Better gas lift allocation by HFPT/LGO results in higher oil production.

value of 8.20 with almost no constraint violation ($< 10^{-8}$). In this case, DGM did not perform as good as LGO.

In Problem 4, the objective function is a sum of condensate and LPG blending at $Plant_6$. In this case, intuitively a good production strategy would be to produce to the other plants as well. Here DGM did outstandingly well, with the values of the objective function in the 124.35 to 131.17, but again while violating the constraint (35) in the order of 0.007. DGM2G found some other 20 stationary points, ranging from 41 to 105. When the constraint (35) is expressed as a polynomial function, DGM2G found the solution with the objective function value 55.85 with almost no constraint violations ($< 10^{-8}$). The consensus value for the objective function

based on the GAMS and LGO solvers is 85.35. However, depending on what is an acceptable degree of constraint violation, there can be many solutions.

Overall, compare with the LGO and the GAMS solvers, the above results are indicative that the DGM2G is a capable global optimization algorithm, less so for DGM1G. To facilitate deployment (not too many knobs for the users) both algorithms were deliberately designed with no user tuneable parameters. The above experience with fractional objective functions and constraints suggests that the DGM is not as robust as LGO when dealing fractional functions.

As the dimension in all problems is small we do not give any detail analysis of other performance indicators.

A more detailed comparative study of the DGM using a large number of real world problems is the subject of our future research. Results with the above test problems demonstrate that LGO and DGM have their own strength; together they can be very useful in production optimization. For engineering applications it is better to have a broad spectrum of global optimization solvers, some methods are more appropriate than others for some special optimization opportunities.

The LGO has now been incorporated into the Shell Hydrocarbon Field Planning Tool (HFPT). Comparative studies of HFPT/LGO against off-the-shelf 3rd party integrated production system software have shown that LGO can come up with better alternative solutions. In the case of a optimal gas lift allocation problem to maximize production [15], the HFPT/LGO combination came up with better gas lift allocation and usage (see Figure 4), which has resulted in better oil production (see Figure 5). At the current oil price of some US$70/barrel, the difference observed may have significant impact on the field development strategy and revenue.

REFERENCES

[1] A.M. Bagirov, *Minimization methods for one class of nonsmooth functions and calculation of semi-equilibrium prices,* in "Progress in Optimization: Contributions from Australasia" (eds: A. Eberhard et al.), Kluwer Academic Publishers, 1999, 147-175.

[2] A.M. Bagirov, *A method for minimization of quasidifferentiable functions,* Optimization Methods and Software, **17(1)**, (2002), 31-60.

[3] A.M. Bagirov, *Continuous subdifferential approximations and their applications,* Journal of Mathematical Sciences, **115**, (2003), 2567-2609.

[4] A.M. Bagirov, M. Ghosh and D. Webb, *A derivative-free method for linearly constrained nonsmooth optimization,* Journal of Industrial and Management Optimization, **2**, (2006), 319-338.

[5] C.C. Barroux, P. Duchet-Suchaux, P. Samier, and R. Nabil, *Linking reservoir and surface simulators: How to improve the coupling solutions*, Society of Petroleum Engineers, **65159**, (2000).

[6] H.P. Benson, and E. Sun, *LGO Versatile tool for global optimization*, OR/MS Today, **27**,(2000), 52-55.

[7] J.R. Cadena, D.J. Schiozer, and A.A. Triggia, *A simple Procedure to Develop Analytical Curves of IPR from Reservoir Simulators with Application in Production Optimization*, Society of Petroleum Engineers, **36139**,(1995).

[8] M.H. Cullender, and R.V. Smith, *Practical Solution of Gas-Flow Equations for Wells and Pipelines with Large Temperature Gradients, Trans.*, American Institute of Mining, Metallurgical, and Petroleum Engineers, **207**, (1956) 281-287.

[9] J.E. Davidson, and B.L. Beckner, *Integrated Optimization for Rate Allocation in Reservoir Simulation*, Society of Petroleum Engineers, **79701**, (2003).

[10] J. Del Rio, R. Camacho, A. Robles, F. Gonzalez,and N. Santamaria, *Nonlinear Multivariate Optimization of Production Systems using a Mechanistic Model*, Society of Petroleum Engineers, **84050**, (2003).

[11] C.A. Floudas, P. Pardalos, C.S. Adjiman, W.R. Esposito, WR., Z.H. Gümüs, S.T. Harding, J.L. Klepeis, C.A. Meyer, and C.A. Schweiger, "Handbook of Test Problems in Local and Global Optimization," Kluwer Academic Press, (1999).

[12] Gas Pipeline Equations. *http : //www.pete.lsu.edu/courses/edwards/pete*4085 */handouts/gas_pipeline_equations.pdf*.

[13] S. Handley-Schachler, C. McKie, and N. Quintero, *New Mathematical Techniques for the Optimisation of Oil & Gas Production Systems*, Society of Petroleum Engineers, **65161**, (2000).

[14] C.A. Haverly, *Studies of the Behavior of Recursion for the Pooling Problem*, SIGMAP Bulletin, Association for Computing Machinery, (1978),
http : //www.gams.com/modlib/libhtml/haverly.htm.

[15] T.L. Mason, A. Bagirov, M van Stiphout, M. Grubmueller, and C. Emelle, *Application of Derivative Free Global Optimization Methods for Production Optimization*, presented at the Shell Reservoir Engineering and Petrophysical Conference, Noordwijk, The Netherlands, September 2005.

[16] Y.D.C Maravi, *New Inflow Performance Relationships for Gas Condensate Reservoirs*, MSc thesis, Texas A&M University, August 2003.

[17] A. Nuemaier, O. Scherbina, W. Huyer and T. Vinkó, *A Comparison of Complete Global Optimization Solvers, HTTP : //www.optimization online.org/db_file/*2004/04/861.pdf

[18] A. Ouenes, S. Bhagavan, P.H. Bunge, and B.J. Travis, *Application of Simulated Annealing and Other Global Optimization Methods to Reservoir Description: Myths and Realities*, Society of Petroleum Engineers, **28415**, (1994).

[19] J.D Pintér, "Global Optimization in Action," Kluwer Academic Publishers, Boston, (1996).

[20] J.D. Pintér, *LGO A Modeling Development System for Continuous Global Optimization. User's Guide*, (2004). Current revision: Pinter Consulting Services, Inc., Halifax, NS, Canada, *http : //www.pinterconsulting.com*.

[21] J.D. Pintér, *Nonlinear Optimization in Modeling Environments. Software Implementations for Compilers, Spreadsheets, Modeling Languages, and Integrated Computing Systems*, in "Continuous Optimization: Current Trends and Applications" (eds: Jeyakumar, V. and Rubinov, A.M.), Springer Science + Business Media, New York, 2006, 147-173.

[22] J.D. Pintér, and F.J. Kampas, *MathOptimizer Professional: Key Features and Illustrative Applications*, in "Global Optimization: From Theory to Implementation" (eds: Liberti, L., and Maculan, N.), 263-279. Springer Science + Business Media, New York, 2006.

[23] Li Qing, An Seungwon, T.W. Gedra, *Solving Natural Gas Loadflow Problems Using Electric Loadflow Techniques, http : //power.ecen.okstate.edu/gedra/gas_loadflow_naps*2003.pdf

[24] G. Steward, A.C. Clark, and S.A McBride, *Field-Wide Production Optimization*, Society of Petroleum Engineers, **59459**, (2001).

[25] P. Wang, M. Litvak, and K. Aziz, *Optimization of Production Operations in Petroleum Fields*, Society of Petroleum Engineers, **77658**, (2002).

[26] Zhou Cheng-Dang, Gao Chu-Qiao, Jin Zhen-Wu, and Wu Xi-Ling, *A Simulated Annealing Approach to Constrained Nonlinear Optimization of Formation Paramaters in Quantitative Log Evaluation*, Society of Petroleum Engineers, **24723**. (1992).

E-mail address: `thomaslicister.Mason@shell.com`

E-mail address: `a.bagirov@ballarat.edu.au`

E-mail address: `jdpinter@hfx.eastlink.ca`